

## UWB IMAGING FOR BREAST CANCER DETECTION USING NEURAL NETWORK

S. A. AlShehri and S. Khatun

Department of Computer and Communication Systems Engineering  
Faculty of Engineering  
University Putra Malaysia  
Serdang, Selangor 43400, Malaysia

**Abstract**—This paper presents a simple feed-forward back-propagation Neural Network (NN) model to detect and locate early breast cancer/tumor efficiently through the investigation of Electromagnetic (EM) waves. A spherical tumor of radius 0.25 cm was created and placed at arbitrary locations in a breast model using an EM simulator. Directional antennas were used to transmit and receive Ultra-Wide Band (UWB) signals in 4 to 8 GHz frequency range. Small training and validation sets were constructed to train and test the NN. The received signals were fed into the trained NN model to find the presence and location of tumor. Very optimistic results (about 100% and 94.4% presence and location detection rate of tumor respectively) have been observed for early received signal components with the NN model. Hence, the proposed model is very potential for early tumor detection to save human lives in the future.

### 1. INTRODUCTION

Breast cancer is one of the main causes of women death [1, 2]. An early detection of tumor existence increases the chances of overcoming the problem. There is large number of detection methods, among them, X-Ray mammography is currently the most widely used [2]. However, this method suffers from high miss detection ratio which can go up to 30% [3] in addition to the damage of surrounding tissues. Another limitation of mammography is its inability to distinguish between malignant and benign tissues [4]. These methods are either expensive and painful or the accuracy in terms of detection and location of the

---

Corresponding author: S. Khatun (Sabira@eng.upm.edu.my).

tumor is not satisfactory [2–4]. These limitations motivate the need for other methods that can overcome such limitations in a cost-effective manner. Microwave Ultra-Wide Band (UWB) imaging is currently the most attractive method [5–10]. This method involves transmitting UWB signals through the breast tissue and records the received signals from different locations. As the dielectric properties of tumor differ from healthy breast tissue, this suggests that the reflected and the scattered signals will be different for both types of tissues [11]. There are two main methods used in UWB [12]: (i) Microwave tomography, in which forward and reversed electromagnetic field equations are solved to detect the location of the tumor; (ii) Transmitting and receiving short pulses using UWB antennas. Both of the above approaches have some drawbacks as either they are unable to detect and locate small tumor size or they must use large number of antennas [7, 8, 13].

To the best of our knowledge, the use of Neural Network (NN) to detect the existence of tumor signature for UWB signals has not been addressed in any open literature. Hence, to overcome the aforementioned shortcomings, we present a method to build a potential NN model for early breast tumor detection efficiently.

This paper is organized as follows. The next section presents the breast model and data collection technique, followed by results and discussions, and finally the conclusion of the paper.

## 2. BREAST MODEL AND DATA COLLECTION

Several different breast model dimensions have been used by researchers [1, 13–16]. We have used a hemisphere shape model with the most common dimensions as presented in Figure 1 and Table 1.

**Table 1.** Model parts sizes.

Model Part	Size (cm)
Breast diameter	10
Breast height	6
Skin thickness	0.2
Chest thickness	2

The dielectric properties that have been used are shown in Table 2 [14] where  $\sigma$  is the tissue conductivity in siemens/meter and  $\epsilon_r$  is the relative permittivity.

In the literature [2, 13, 15–20] the tumor radius size ranges from

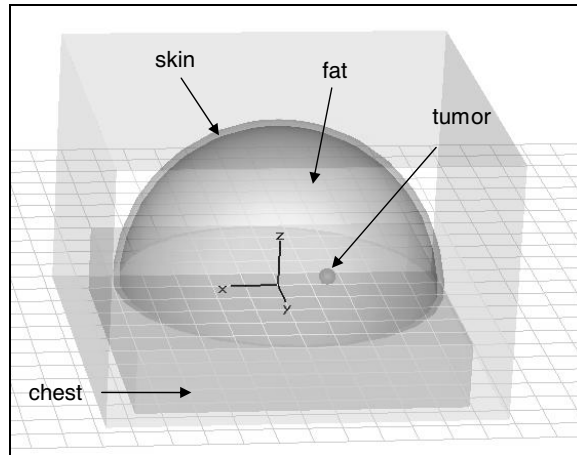


**Figure 1.** A simple breast and tumor model.

**Table 2.** Dielectric properties of the model components at 4 GHz.

	Conductivity $\sigma$ (S/M)	Permittivity $\epsilon_r$
Skin	1.49	37.9
Fat	0.14	5.14
Chest	1.85	53.5
Tumor	1.20	50.0

0.2 cm to about 1.5 cm or more, but 0.25 cm is the mostly used one. We have used a spherical tumor with radius 0.25 cm to compare our results with other related works as it is more common in the literature. Also, it is close to the minimum used tumor size. In future, we will study the use of smaller sizes in our NN model. The dielectric property of the tumor tissue varies with the change of frequency while it remains almost constant for the healthy and fat tissues [15, 16, 21]. This property motivates the use of frequencies 4 and 8 GHz as center frequencies. Frequency 4 GHz is centered between [3 to 5 GHz] and 8 is centered between [7 to 9 GHz]. To generate the data, we used the following steps:

- 1) Place a pair of transmitter-receiver at opposite sides of the breast model in a line.
- 2) Place a tumor at any location ' $l$ ' along the  $x$ -axis in the model.

- 3) Transmit first a 4 GHz (center frequency) signal using plane wave located in  $x$ -axis direction.
- 4) Receive the signal on the opposite side.
- 5) Change tumor location and repeat (2–4) a number of times.
- 6) The above steps were repeated for 8 GHz (center frequency).

This data generation procedure was conducted for 19 different locations by placing the tumor along  $x$ -axis. Also, the model without the tumor tissue was used three times to get the propagated signals through healthy breast. The Transmitter (Tx) and Receiver (Rx) are separated by only 10 cm (breast diameter). So, noise is negligible and not considered here.

The emitted (transmitted) EM waves (UWB) usually travel in 3-D. Hence if there is any tumor (or scattering object) in the breast model, the receiver must receive scattered signal in addition to normal reception regardless of the tumor's location. Also, in our system, the Tx-Rx pair is rotated  $360^\circ$  for full 2-D detection and to extend the 1-D case to 2-D. During this  $360^\circ$  rotation, the tumor (if any) should be along the line between Tx-Rx twice (one direct and the other one is complement ( $180^\circ$  phase difference)). Hence, it is enough to train the NN by placing the tumor along the  $x$ -axis (one dimension) only.

This experiment was repeated by placing the tumor along the  $y$ -axis and transmitting the signals from plane facing the  $y$ -axis to get 6 different received signals for testing purposes. The same experiment was conducted twice without placing tumor for testing too. As a result, three groups of received signals were formed as follows:

**Group (1):** a set of 18 signals (16 with tumor and 2 without tumor along  $x$ -axis) were feed into the NN model to train the model for efficiently detecting and locating purposes.

**Group (2):** a set of 4 signals (3 with tumor and 1 without tumor along  $x$ -axis) were used to validate the NN.

**Group (3):** a set of 8 signals (6 with tumor and 2 without tumor along  $y$ -axis) were feed into the trained NN model to test its detection efficiency.

The whole experiment was done for both 4 and 8 GHz. The 8 GHz transmitted signal and one received UWB signal are shown in Figure 2.

### 3. TUMOR DETECTION USING FEED-FORWARD NEURAL NETWORK

#### 3.1. Detection along One Dimension (1-D)

In the received signals (Figure 2), according to EM simulator which is CST software [22], the data points can go between 4500 to 7200 points.

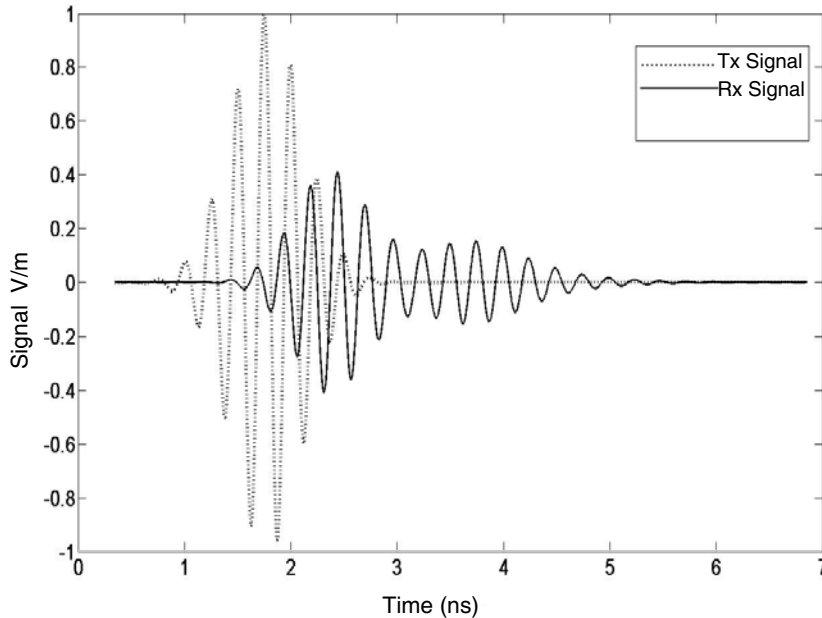


**Figure 2.** The 8 GHz transmitted and a corresponding received UWB signal in electromagnetic simulator.

The signal propagation time is computed by the EM simulator. The signature of the tumor is hidden in these data. Neural Network is one of the best tools in such recognition application though the best NN architecture and learning algorithm is a very difficult problem [17, 23–27]. The most used methods to overcome this problem are network growing and pruning techniques. These techniques depend on expanding or shrinking the NN size until a reasonable output is obtained [21]. We used the network growing technique and variety of NN architectures with different learning algorithms. Due to limited training and testing data set, we used feed-forward back-propagation NN as it is efficient for such data sets. The NN model was implemented in MATLAB with two hidden layers. The first layer has 20 nodes and the second layer has 7 nodes. Only one node is needed in the output layer since the output of the NN is the location of the tumor or ‘-1’ if it does not exist. After many trials, we found that this NN architecture showed the best performance for this kind of application. Figure 3 shows the NN schematic while Table 3 shows the NN MATLAB training parameters. The used transfer function is “tansig” which has output in the range  $[-1, +1]$ . The training function is “traingdm”

which is gradient descent with momentum back-propagation.

For the proposed NN model, the error ( $E$ ) is calculated as follows:

$$MSE = \frac{1}{2} \sum_j (t_j - y_j)^2 \quad (1)$$

where,  $t$  is the actual target,  $y$  is the net output and  $j$  is number of output units. But for the proposed NN model, the error ( $E$ ) is calculated as follows:

$$E = \frac{1}{n} \sum_n (t_n - y_n) \quad (2)$$

where  $t$  is the actual target,  $y$  is the net output and  $n$  is the number of NN input samples which were generated using EM simulator. The feature vector contains the signal data points which constitute the patterns for the NN training. The output is the distance between the center of the tumor and the outer surface of the skin on the  $x$ -axis direction as shown in Figure 1. To generate pattern feature vectors we used the following procedures:

- 1) Interpolate the data using “shape-preserving piecewise cubic interpolation” to generate fixed time step.
- 2) Combine all data signals within 4 to 8 GHz with tumor.
- 3) Insert signals received when tumor is not present in the breast model.
- 4) Shuffle the signal order in the feature vector for NN generalizing purposes.
- 5) Generate the target vector dividing by 10 (breast diameter) to limit the values to be less than 1. This is because the transfer function “tansig” has output in the range  $[-1, +1]$ .

Since the data points are large and the training set is small, the problem of overfitting may arise. To solve this problem, some of the signals were used to form a validation test data (Group 2). The training of the NN was repeated a large number of time to reach the best results and to overcome overfitting problems.

### 3.2. Detection in Two Dimension (2-D)

Referring to Figure 4, to detect the existence of a tumor in 2-D we apply the same simulation steps as 1-D. The NN obtained in the 1-D training step is used. Transmitter (Tx) and Receiver (Rx) are rotated around  $360^\circ$  at  $1^\circ$  step size. For example, if the location performance accuracy is  $X\%$ , this gives  $(100 - X)\%$  error, then the locating error,

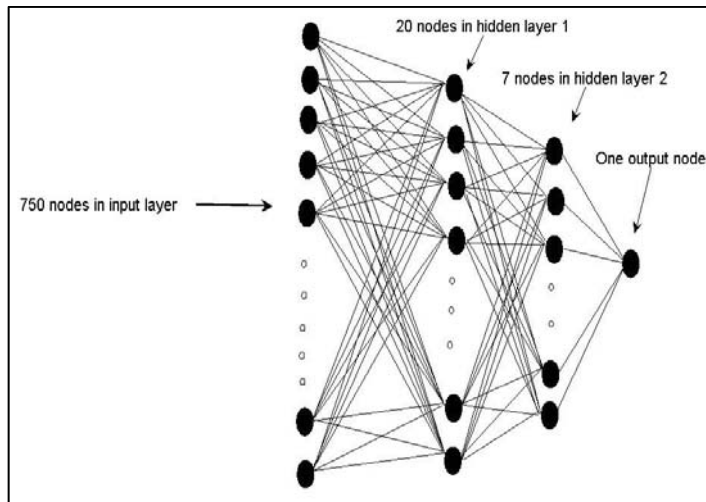


**Figure 3.** The NN model schematic.

**Table 3.** NN parameters used in MATLAB training.

NN parameters used in MATLAB	Values
number of nodes in Input layer	750
number of nodes in Hidden layer 1	20
number of nodes in Hidden layer 2	7
number of nodes in Output layer	1
Transfer function	tansig
Training function	traingdm
Learning rate	0.005
Momentum constant	0.9
Maximum no. of Epochs	400000
Minimum performance gradient	1e-25

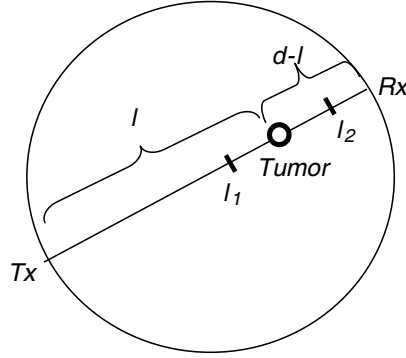


**Figure 4.** Layout of 2-D detection.

$er = \pm(100 - X)/2$ . If a tumor is found at a location  $l$  when Tx and Rx are placed at an angle  $\theta^\circ$ , then

$$l = \begin{cases} \min(l_2^\theta) = \frac{l}{1-er} \\ \max(l_1^\theta) = \frac{l}{1+er} \\ \text{between them.} \end{cases} \quad (3)$$

as shown in Figure 4. Here,  $l_1^\theta$  and  $l_2^\theta$  are the two possible distances of tumor from Tx when Tx-Rx pair is situated at an angle  $\theta$ . To confirm the location, we would expect to find a tumor signature at the complement distances when the Tx-Rx pair is rotated at an angle  $180^\circ$ . The two ranges become:

$$l = \begin{cases} \min(l_2^{\theta+180}) = \left(d - \frac{l}{1-er}\right) \pm er \left(d - \frac{l}{1-er}\right) & (4) \\ \max(l_1^{\theta+180}) = \left(d - \frac{l}{1+er}\right) \pm er \left(d - \frac{l}{1+er}\right) & (5) \end{cases}$$

Here,  $d$  is the diameter of the breast model. From Equations (3) and (4) a tumor should be detected and located on the opposite side between  $d(1-er) - l$  and  $d(1+er) - l$ . Otherwise, there is no tumor along this diameter at angle  $\theta$ .

To test and proof Equations (3) and (4), a tumor was placed at  $l = 7.5$  cm with  $d = 10$  cm. The developed NN model accuracy is approximately 94.4% (This is presented and discussed in details in Section 4). Using this accuracy result,  $er\% = \left(\frac{100-94.4}{2}\right)\%$ . Form the same  $l$  using Equations (3) and (4), a tumor can be detected in between  $l_2 = 2.22$  cm and  $l_1 = 2.78$  cm from other side of the diameter.

Using the NN model, we detected the same tumor at approximated distance  $l = 6.8$  cm. After rotating the Tx-Rx pair by  $180^\circ$ , the tumor is supposed to be detected at  $l = 2.5$  cm as an exact location. But the NN model has detected the tumor at  $l' = 2.9$  cm, where Equations (4) and (5) give the value as  $l' = 2.78$  cm. The both values are very close and hence acceptable.

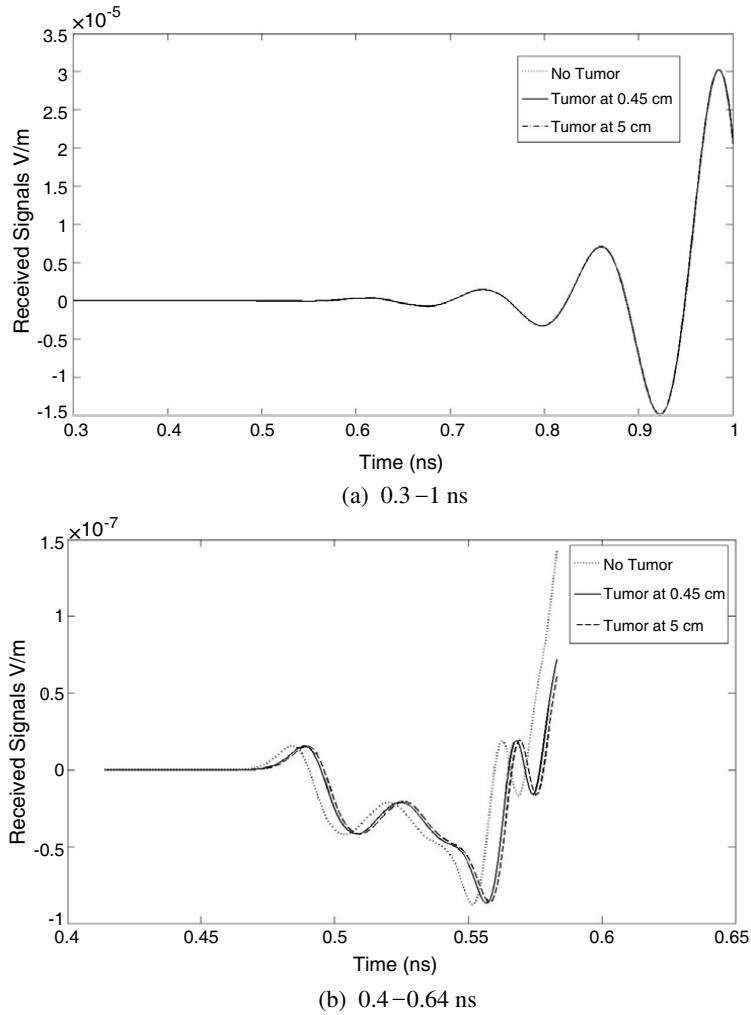


**Figure 5.** Three received signals in times between (a) 0.3–1 ns and (b) 0.4–0.65 ns.

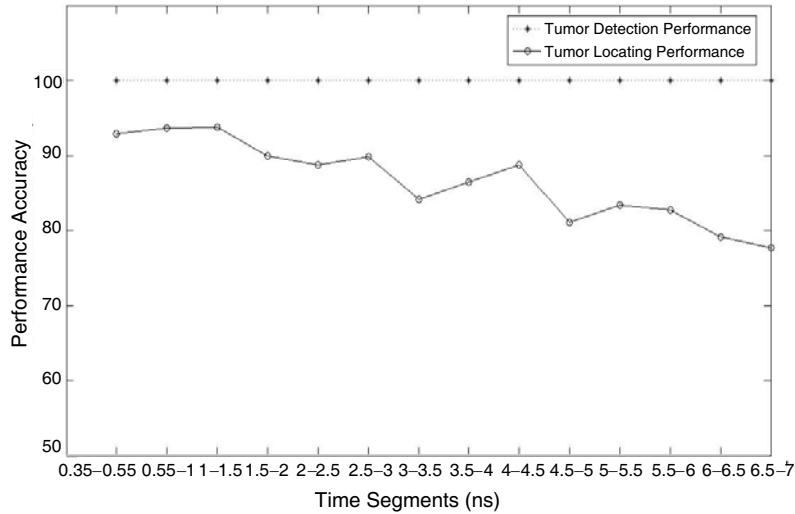


**Figure 6.** Tumor detection and locating performance result for different time segments.

#### 4. RESULTS

The network growing technique was used to obtain the best NN size. We have tried all possible combinations of our data signals from 4 to 8 GHz (center frequencies) with the trained NN model. The data points of a given signal were segmented and then used. For example, data points were segmented for the range from time duration 0.35 ns to 1 ns, from 1 ns to 2 ns and so on. This was done for all signals to increase the detection efficiency and accuracy. By looking (Figure 5) at the early stage received signal value (for example 0.4–0.65 ns), a variation in the received signals can be recognized, which contains some tumor signature. Figure 5 shows three received signals with variations. The best performance is obtained for the signal points in the range from 0.45 ns to about 0.6 ns. This happens due to the fact that, the direct signal path components arrive at the receiver at an early stage which gives pure signal reception. As time goes, the scattered and reflected signals components caused by the tumor object are accumulated at the receiver which causes the lately received signal not to be pure enough to show the existence of tumor signature.

Figure 6 shows the detection accuracy of the presence of tumor and its location by NN model. It shows that nearly full detection rate ( $\sim 100\%$ ) can be achieved. The detail can be seen by looking

at the NN output presented in Table 4. If the output is negative, this means that there is no tumor. Table 4 confirms that for each negative input, NN output is negative, whereas positive inputs give positive outputs, showing its detection efficiency. Also, it shows some variations in terms of tumor location. Tumors in radius equal to 0.2 cm and 0.3 were correctly detected but with relatively large location errors. This is due to the fact that the NN was not trained on different tumor radius sizes. Table 5 shows the segmented time scale training and validation performance of the NN model. The training, validation and testing percentages accuracy were calculated using Equation (1) for Groups (1), (2) and (3) signals. It can be observed that the time segment (0.35–1 ns for 4 to 8 GHz) gives the best performance and the three accuracy percentages were nearly equal. The average location accuracy is nearly 94.4% for testing purposes.

**Table 4.** Actual tumor locations and the NN output for tumor placed on  $y$ -axis where  $x$ -axis and  $z$ -axis are fixed at 0 and 0.25 cm respectively.

Actual tumor location (cm/10) in EM simulator	NN output (cm/10)
0.15	0.04
-1.0	-0.97
0.43	0.41
0.70	0.50
-1.0	-0.97
0.25	0.28
0.60	0.61
0.65	0.649
0.86	0.84

The trained NN (with tumor size 0.25 cm) was tested for two other sizes (0.2 cm and 0.3 cm) for performance verification. The NN is able to detect the presence of tumor in both cases. But it shows relatively higher error to find the tumor location. It exhibits higher error for 0.3 cm than 0.2 cm tumor size. For example, a tumor with radius 0.2 cm was detected by the NN at  $l = 7.7$  cm whereas it was placed at  $l = 4.5$  cm.

Similar and complete performance measure was not found in previous studies. However, it has been reported in an experimental

**Table 5.** Location accuracy comparison for data different time segments.

Data in Time Segments	% Training Accuracy	%Validation Accuracy	% Testing Accuracy
0–7 ns, 4 GHz	99.6	89.2	86.0
0–4.3 ns, 8 GHz	99.2	93.5	92.2
0.35–1 ns, 4 GHz	85.2	91.0	92.2
0.35–1 ns, 8 GHz	87.1	92.3	94.6
<b>0.35–1 ns, 4, 8 GHz</b>	<b>95.4</b>	<b>96.8</b>	<b>94.4</b>
1–2 ns, 4, 8 GHz	90.3	90.5	92.9
2–3 ns, 4, 8 GHz	94.1	88.4	88.7
3–4 ns, 4, 8 GHz	99.6	91.1	87.9
4–5 ns, 4, 8 GHz	98.5	82.1	82.5
5–6 ns, 4, 8 GHz	98.1	90.1	85.5
6–7 ns, 4, 8 GHz	84.7	87.4	86.0

work that, a tumor at actual location of 6.5 cm was successfully located at 6.06 cm [18]. This resulted in a relative error of 6.77% which gives locating accuracy of 93.2%. Using the proposed NN model, a tumor located at the same location was located with accuracy of 99.8%. This shows 6.6% improvement of the proposed NN model (in both cases noise is negligible).

## 5. CONCLUSION AND FUTURE WORKS

A feed-forward NN model is developed to identify the existence and location of tumor tissue in a breast model. This work was successfully done for 1-D and 2-D slice of the 3-D breast model with a tumor size of 0.25 cm in radius. UWB signals were used to construct the feature vector patterns for 4 to 8 GHz center frequencies range. The NN model is able to detect the presence of tumor successfully. The detection performance could reach up to 100% showing its efficiency. At the same time, it is able to find out the tumor location with average accuracy 94.4%. This model shows also that early stage received signals (0.35–1 ns) are enough to detect and locate the tumor signature. A full 3-D breast model with variant tumor size and large data samples is currently on-going to detect and locate the cancer in very early stage. Discrimination between malignant and benign tissues

is currently under investigation. More complex and realistic breast model can also be tested using this method.

## REFERENCES

1. Shao, W. and B. Zhou, "UWB microwave imaging for breast tumor detection in inhomogeneous tissue," *Proceedings of the 2005 IEEE Engineering in Medicine and Biology, 27th Annual Conference, Shanghai, China*, 1496–1499, 2005.
2. Sill, J. M. and E. C. Fear, "Tissue sensing adaptive radar for breast cancer detection-experimental investigation of simple tumor models," *IEEE Transactions on Microwave Theory and Techniques*, Vol. 53, 3312–3319, 2005.
3. Huynh, P. T., A. M. Jarolimek, and S. Daye, "The false-negative mammogram," *Radiograph*, Vol. 18, 1137–1154, 1998.
4. Huo, Y., R. Bansal, and Q. Zhu, "Breast tumor characterization via complex natural resonances," *IEEE MTT-S International Microwave Symposium Digest*, Vol. 18, 387–390, 2003.
5. Paulsen, K. D. and P. M. Meaney, "Nonactive antenna compensation for fixed-array microwave imaging — Part I: Model development," *IEEE Transactions on Medical Imaging*, Vol. 18, 496–507, 1999.
6. Meaney, P. M., K. D. Paulsen, J. T. Chang, M. W. Fanning, and A. Hartov, "Nonactive antenna compensation for fixed-array microwave imaging — Part II: Imaging results," *IEEE Transactions on Medical Imaging*, Vol. 18, 508–518, 1999.
7. Fear, E. C., S. C. Hagness, P. M. Meaney, M. Okoniewski, and M. A. Stuchly, "Enhancing breast tumor detection with near-field imaging," *IEEE Microwave Magazine*, Vol. 3, 48–56, 2002.
8. Bond, E. J., X. Li, S. C. Hagness, and B. D. Van Veen, "Microwave imaging via space-time beam forming for early detection of breast cancer," *IEEE Trans. Antennas Propag.*, Vol. 51, 1690–1705, 2003.
9. Li, X., S. K. Davis, S. C. Hagness, D. W. Weide, and B. D. Veen, "Microwave imaging via space-time beam forming: Experimental investigation of tumor detection in multilayer breast phantoms," *IEEE Trans. Microwav. Theory Tech.*, Vol. 52, 1856–1865, 2004.
10. Shannon, C., E. Fear, and M. Okoniewski, "Dielectric-filled slotline bowtie antenna for breast cancer detection," *Electronics Letters*, Vol. 41, 388–390, 2005.
11. Sha, L., E. R. Ward, and B. Story, "A review of dielectric

- properties of normal and malignant breast tissue,” *Proceedings IEEE SoutheastCon*, 457–462, 2002.
12. Abbosh, A. M. and M. E. Bialkowski, “Design of UWB planar for microwave imaging systems,” *IEEE International Conference on Signal Processing and Communications (ICSPC 2007)*, 24–27, Dubai, United Arab Emirates, 2007.
  13. Fear, E. C. and M. A. Stuchly, “Microwave detection of breast cancer,” *IEEE Transactions on Microwave Theory and Techniques*, Vol. 48, 1854–1863, 2000.
  14. Miyakawa, M., T. Ishida, and M. Wantanabe, “Imaging capability of an early stage breast tumor by CP-MCT,” *Proceedings of the 26th Annual International Conference of the IEEE EMBS*, Vol. 1, 1427–1430, San Francisco, CA, USA, 2004.
  15. Wang, M., S. Yang, S. Wu, and F. Luo, “A RBFNN approach for DoA estimation of ultra wideband antenna array,” *Neurocomputing*, Vol. 71, 631–640, 2008.
  16. Klemm, M., I. Craddock, J. Leendertz, A. Preece, and R. Benjamin, “Experimental and clinical results of breast cancer detection using UWB microwave radar,” *Proceedings of IEEE Antennas and Propagation Society International Symposium*, 1–4, 2008.
  17. Lim, H. B., N. T. Nhung, E. Li, and N. D. Thang, “Confocal microwave imaging for breast cancer detection: Delay-multiply-and-sum image reconstruction algorithm,” *IEEE Transaction on Biomedical Engineering*, Vol. 55, 1697–1704, 2008.
  18. Bindu, G., A. Lonappan, V. Thomas, C. K. Anadan, and K. T. Mathew, “Active microwave imaging for breast cancer detection,” *Progress In Electromagnetic Research, PIER* 58, 149–169, 2006.
  19. Fear, E. C., J. Still, and M. A. Stuchly, “Experimental feasibility study of confocal microwave imaging for breast tumor detection,” *IEEE Transactions on Microwave Theory and Techniques*, Vol. 51, 887–897, 2003.
  20. Davis, S. K., H. Tandradinata, S. C. Hagness, and B. D. Veen, “Ultrawideband microwave breast cancer detection: A detection-theoretic approach using the generalized likelihood ratio test,” *IEEE Transactions on Biomedical Engineering*, Vol. 52, 1237–1250, 2005.
  21. Lazebnik, M., et al., “A large-scale study of the ultrawideband microwave dielectric properties of normal, benign and malignant breast tissues obtained from cancer surgeries,” *IOP PUBLISHING, Phys. Med. Biol.*, Vol. 52, 6093–6115, 2007.

22. CST MICROWAVE STUDIO, CST inc., 2008.
23. Bishop, C. M., *Neural Networks for Pattern Recognition*, Oxford University Press, 1997.
24. Zhang, Y. and L. Wu, "Weights optimization of neural network via improved BCO approach," *Progress In Electromagnetic Research*, PIER 83, 185–198, 2008.
25. Shiva Nagendra, S. M. and Mukesh Khare, "Artificial neural network approach for modeling nitrogen dioxide dispersion from vehicular exhaust emissions," *Elsevier, Ecological Modeling*, Vol. 190, 99–115, 2006.
26. Messer, K. and J. Kittler, "Choosing an optimal neural network size to aid a search through a large image database," *Proceedings of the Ninth British Machine Vision Conference, BMVC 98*, 1998.
27. Wang, L. and H. Quek, "Optimal size of a feedforward neural network: How much does it matter?" *IEEE, Proceedings of the Joint International Conference on Autonomic and Autonomous Systems and International Conference on Networking and Services (ICAS/ICNS 2005)*, 2005.